

Supporting Information

Uniting Young's Modulus and Flexibility of Solid-State Electrolyte for High-Performance Li-Batteries at room temperature

Haitao Zhao¹, Yan Zhang¹, Zehua Zhao¹, Zhuangzhuang Xue¹, and Lei Li^{1*}

¹State Key Laboratory for Mechanical Behavior of Materials, Xi'an Jiaotong

University, No.28, Xianning West Road, Xi'an, Shaanxi, 710049, China

Email: l-li@xjtu.edu.cn

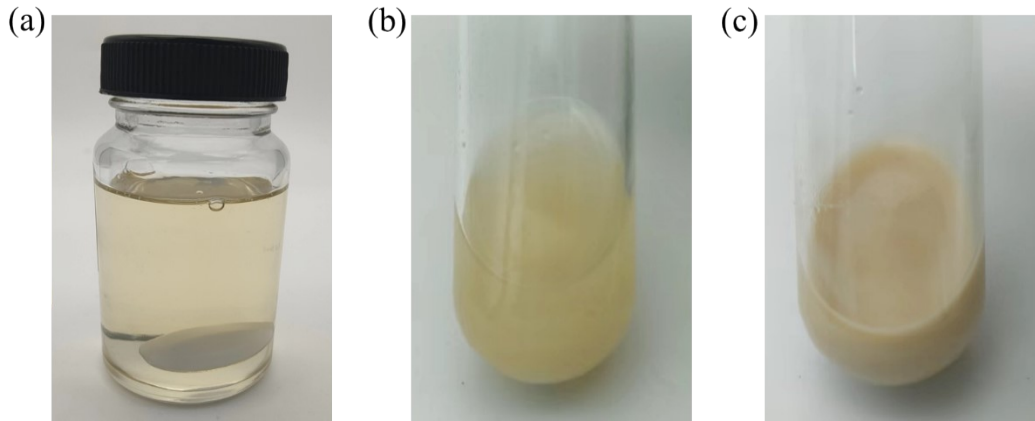


Fig. S1. Digital images of (a) SPE solution, (b) CIP slurry, (c) PIC slurry.

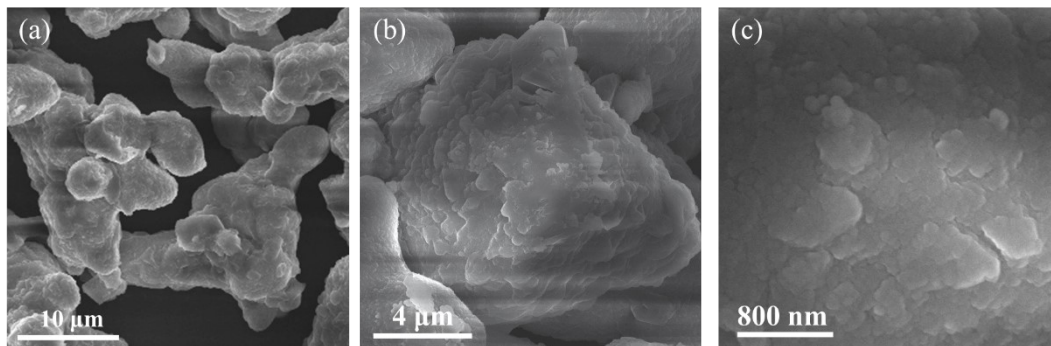


Fig. S2. (a-c) FE-SEM image of LLZTO particles at different magnification.

As shown in Fig. S2a, LLZTO was an irregular particle. And the surface of LLZTO particles was scaly (Fig. S2b,c).

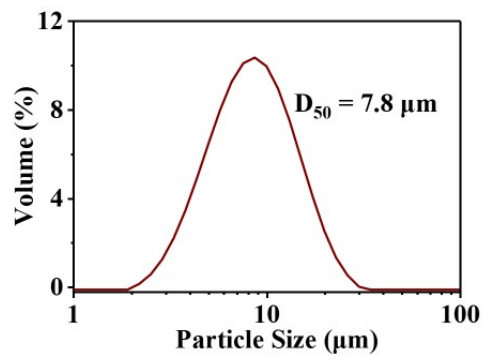


Fig. S3. The particle size distribution of LLZTO particles. The D_{50} of LLZTO is 7.8 μm.

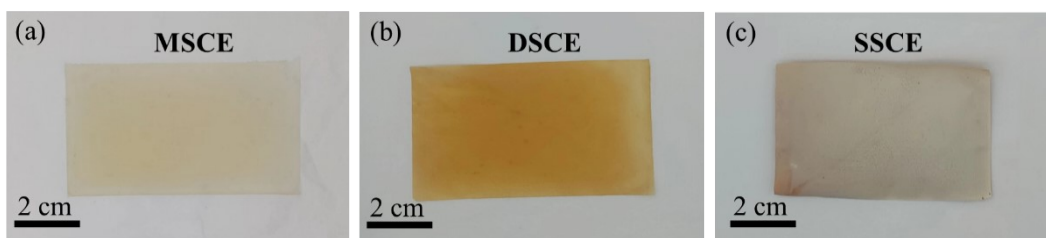


Fig. S4. Digital images of (a) MSCE, (b) DSCE, and (c) SSCE.

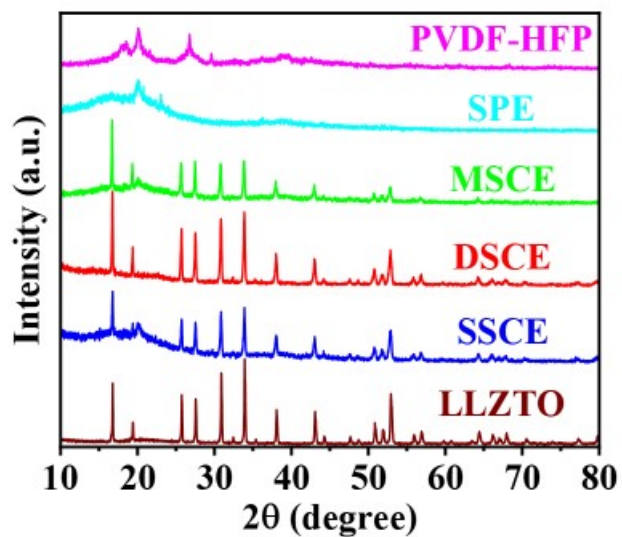


Fig. S5. XRD patterns of PVDF-HFP, SPE, MSCE, DSCE, SSCE and LLZTO particles.

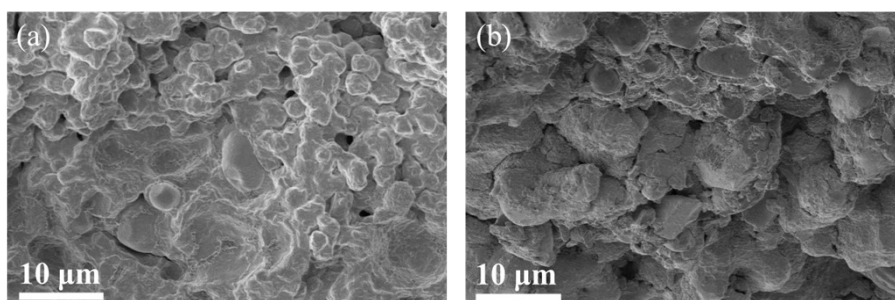


Fig. S6. Cross-sectional FE-SEM images of (a) the interphase between PIC layer and CIP layer, (b) the PIC layer in SSCE.



Fig. S7. Digital image of fractured, incomplete PIC with extremely poor flexibility.

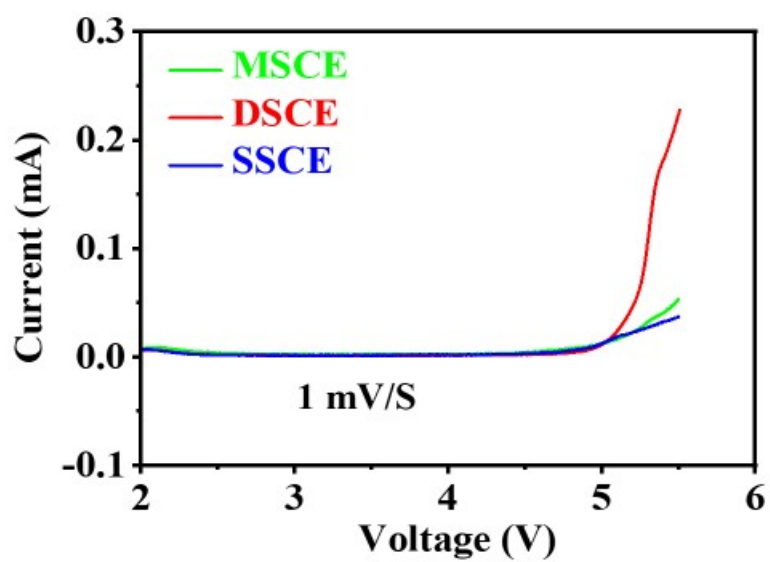


Fig. S8. Linear sweep voltammogram curves of MSCE, DSCE and SSCE.

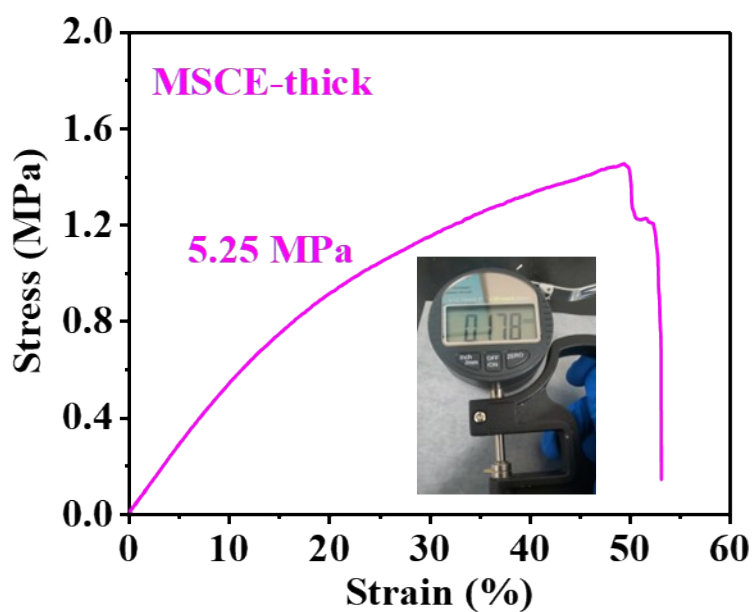


Fig. S9. Stress–strain curves and Digital image of the thickness of MSCE-thick.

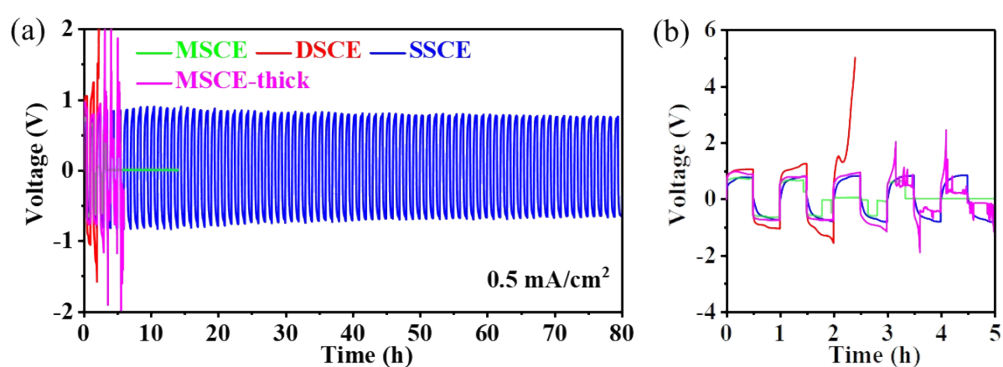


Fig. S10. Galvanostatic cycling measurements of Li|MSCE|Li, Li|DSCE|Li, Li|SSCE|Li and Li|MSCE-thick|Li at 0.5 mA/cm² with 0.5 h stripping and 0.5 h plating per cycle. (a) The voltage profiles, and (b) local view of voltage profiles at 0-4 h.

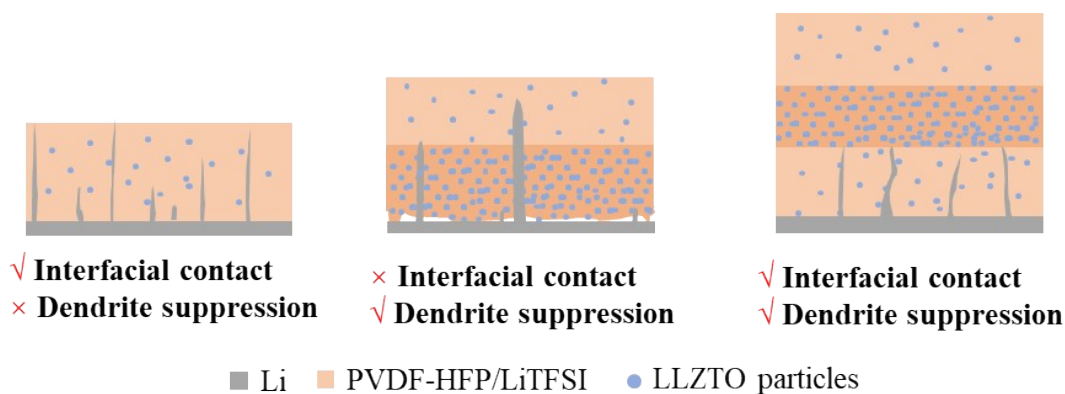


Fig. S11. Schematic illustration of MSCE, DSCE and SSCE suppressing Li dendrite growth and enhancing contact with electrodes.

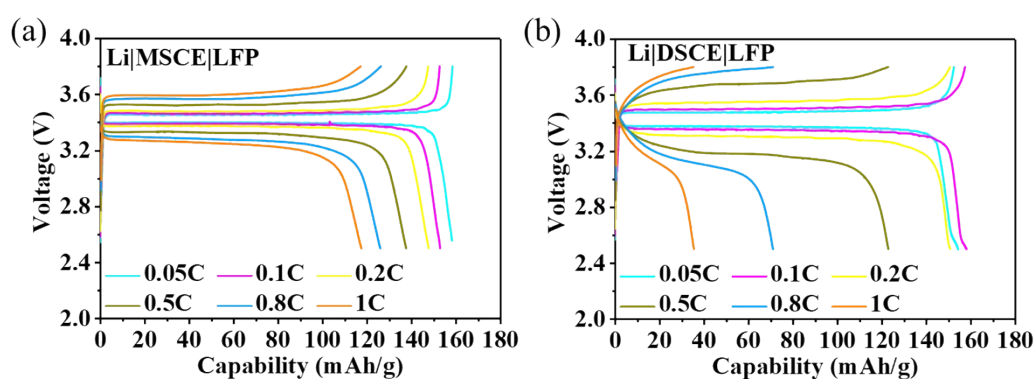


Fig. S12. Charge/discharge curves of (a) Li|MSCE|LFP; and (b) Li|DSCE|LFP at various current rates from 0.05 to 1C at 25 °C.

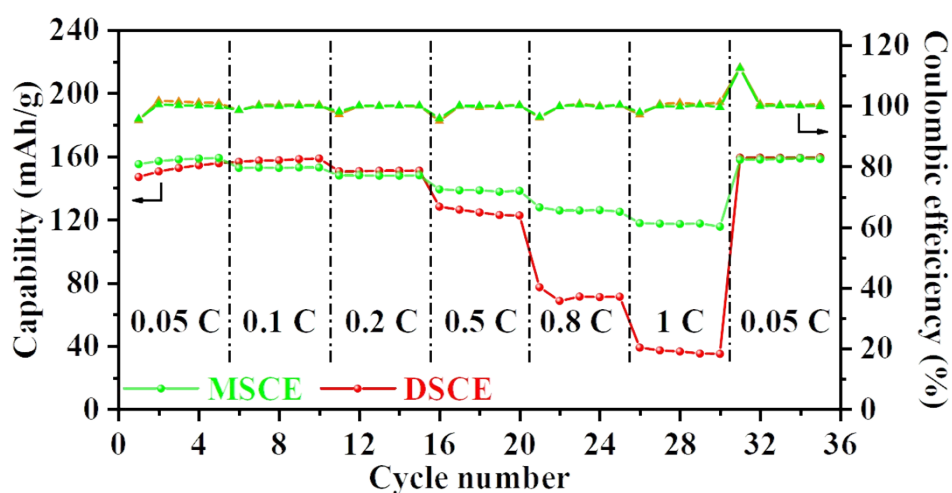


Fig. S13. The rate performance of Li|MSCE|LFP and Li|DSCE|LFP at various current rates from 0.05 to 1C at 25 °C.

Table S1. Comparisons of ionic conductivity solid-state electrolytes and cycling performance of all-solid-state batteries using LiFePO₄ as cathode active material.

solid-state electrolytes	working temperature (°C)	ionic conductivity (10 ⁻⁴ S/cm)	voltage range (V)	rate	initial discharge capacity (mA h/g)	capacity retention (%)	ref.
SSCE	25	4.57	2.5-3.8	0.5C	130.3	98.8 (450 cycles)	This work
sandwich structure PEO/PVDF-HFP@LLZTO/PEO	40	2.86	2.5-4.0	0.2C	147.2	83.6 (140 cycles)	S1
sandwich structure PEO@20 vol% LLZTO/PEO@80 vol% LLZTO/PEO@20 vol% LLZTO	30	1.60	2.8-3.8	0.1C	120	82.4 (200 cycles)	S2
the electrospun sandwich-like membrane PVDF-HFP/PAN/PVDF-HFP	30	2.15	2.8-4.0	0.5C	120	82 (400 cycles)	S3
sandwich structure PPC/polypropylene separator /PPC@SN	25	2.18	2.6-4.2	0.1C	140	/	S4
sandwich structure PVDF/polypropylene separator /PVDF	25	1.53	2.8-3.6	0.3C	134	97.8 (140 cycles)	S5
monolayered structure PVA@PAN@20 wt % LATP @ 10 wt% SN	25	1.13	2.0-4.0	0.5C	119.4	90.5 (100 cycles)	S6

- [S1] Z. Xie, Z. Wu, X. An, X. Yue, P. Xiaokaiti, A. Yoshida, A. Abudula and G. Guan, *J. Membr. Sci.*, 2020, **596**, 117739.
- [S2] H. Huo, Y. Chen, J. Luo, X. Yang, X. Guo and X. Sun, *Adv. Energy Mater.*, 2019, **9**, 1804004.
- [S3] D. Zhang, X. Xu, S. Ji, Z. Wang, Z. Liu, J. Shen, R. Hu, J. Liu and M. Zhu, *ACS Appl. Mater. Interfaces*, 2020, **12**, 21586-21595.
- [S4] H. Yue, J. Li, Q. Wang, C. Li, J. Zhang, Q. Li, X. Li, H. Zhang and S. Yang, *ACS Sustainable Chem. Eng.*, 2018, **6**, 268-274.
- [S5] K. Shi, Z. Xu, M. Huang, L. Zou, D. Zheng, Z. Yang and W. Zhang, *J. Membr. Sci.*, 2021, **638**, 119713.
- [S6] H. K. Tran, Y.-S. Wu, W.-C. Chien, S.-h. Wu, R. Jose, S. J. Lue and C.-C. Yang, *ACS Appl. Energy Mater.*, 2020, **3**, 11024-11035.